Jpn. J. Appl. Phys. Vol. 38 (1999) pp. 3976–3981
Part 1, No. 7A, July 1999

Characteristics of InGaN-Based UV/Blue/Green/Amber/Red Light-Emitting Diodes

Takashi MUKAI, Motokazu YAMADA and Shuji NAKAMURA
Department of Research and Development, Nichia Chemical Industries Ltd., 491 Oka, Kaminaka, Anan, Tokushima 774-8601, Japan

(Received February 15, 1999; accepted for publication April 5, 1999)

Highly efficient light-emitting diodes (LEDs) emitting ultraviolet (UV), blue, green, amber and red light have been obtained through the use of InGaN active layers instead of GaN active layers. Red LEDs with an emission wavelength of 675 nm, whose emission energy was almost equal to the band-gap energy of InN, were fabricated. The dependence of the emission wavelength of the red LED on the current (blue shift) is dominated by both the band-filling effect of the localized energy states and the screening effect of the piezoelectric field. In the red LEDs, a phase separation of the InGaN layer was clearly observed in the emission spectra, in which blue and red emission peaks appeared. In terms of the temperature dependence of the LEDs, InGaN LEDs are superior to the conventional red and amber LEDs due to a large band offset between the active and cladding layers. The localized energy states caused by In composition fluctuation in the InGaN active layer contribute to the high efficiency of the InGaN-based emitting devices, in spite of the large number of threading dislocations and a large effect of the piezoelectric field. The blue and green InGaN-based LEDs had the highest external quantum efficiencies of 18% and 20% at low currents of 0.6 mA and 0.1 mA, respectively.

KEYWORDS: InGaN, GaN, LEDs, blue, green, amber, SQW, ELOG, dislocations

1. Introduction

Light-emitting diodes (LEDs) are the ultimate solid-state light sources. At present, incandescent bulbs and fluorescent lights are used as light sources for many applications. However, these conventional light sources are traditional glass-vacuum-type light sources with poor reliability and durability and a low luminous efficiency. In the past, electronic circuits were made of glass vacuum tubes in spite of their poor reliability and durability. Now, all electronic circuits are highly reliable solid-state semiconductor circuits. Thus, only light sources are still made using old technology. The applications of the LEDs have been limited, however, by the lack of materials that can efficiently emit blue and green light. Full-color displays, for example, require at least three primary colors, usually red, green and blue, to produce any visible color. Such a combination is also needed to make a white-light-emitting device that would be more durable with less power consumption than conventional incandescent bulbs or fluorescent lights. Recently, III-V nitride-based materials have opened the way to a realization of high-efficiency uv/blue/green/amber LEDs.

III-V nitride-based semiconductors have a direct band gap that is suitable for blue-light-emitting devices. The band-gap energy of aluminum gallium indium nitride (AlGaInN) varies between 6.2 and 1.89 eV, depending on its composition, at room temperature (RT). Thus, by using these semiconductors, red- to ultraviolet-emitting devices can be fabricated. In 1992, our group[1] succeeded, for the first time, in growing high-quality InGaN films which exhibited a strong band-to-band emission from the green to UV range, by changing the In content of InGaN using a novel two-flow metalorganic chemical vapor deposition (MOCVD) method. Also, Nakamura et al. fabricated the first InGaN/GaN double-heterostructure (DH) LEDs in 1993.[2] Finally, they were able to grow an InGaN multi-quantum-well (MQW) structure, and confirmed an enhanced strong photoluminescence (PL) intensity from quantized energy levels of the InGaN well layer with a thickness of 25 Å, for the first time.[3] A small amount of indium added to the GaN is essential for obtaining a strong band-to-band emission because GaN without indium does not emit a strong band-to-band emission at RT. The reason for this is considered to be related to deep localized energy states caused by In composition fluctuation.[4–8]

Using the InGaN active layer described above, in 1994, Nakamura *et al.*[9] developed the first blue InGaN/AlGaN double-heterostructure LEDs this was followed in 1995 by the blue/green InGaN single-quantum-well (SQW) structure LEDs.[10] Then, UV/amber LEDs[11–13] and the first demonstration of RT violet laser light emission in InGaN-MQW/GaN/AlGaN-based heterostructures under pulsed operations were achieved.[14] All of these light-emitting devices utilize an InGaN active layer instead of a GaN active layer, because it is difficult to fabricate a highly efficient light-emitting device using a GaN active layer, the reason for which is still not clear. Also, the InGaN active layer in these LEDs includes a large number, from 1×10^8 to 1×10^{12} cm^{-2}, of threading dislocations (TDs) originating from the interface between GaN and the sapphire substrate due to a large lattice mismatch of 13.5%.[15] The TDs are considered to be formed as a result of a complex set of interactions involving, for example, the interface energy, the nucleation density and the island coalescence.[16,17] In spite of this large number of dislocations, the efficiency of the InGaN-based LEDs is almost equal to or higher than that of the conventional III-V compound semiconductor (AlGaAs and AlInGaP)-based LEDs. In many conventional optoelectronic devices, the device performance has been limited by controlling both point defects and structural defects in these materials. However, these recent reports now suggest that III-V nitride-based devices are less sensitive to dislocations than conventional III-V semiconductors.

Chichibu *et al.*[18] studied the emission mechanisms of GaN and InGaN quantum wells (QWs) by comparing their optical properties as a function of TD density, which was controlled by the lateral epitaxial overgrowth (LEO) technique. PL intensity was slightly strengthened by reducing the TD density from 1×10^{10} cm^{-2} to nearly zero (less than 1×10^6 cm^{-2}). Also, the major PL decay time was independent of the TD density. These results suggested that the emission mechanisms are unaffected by TDs. TDs are considered to simply reduce the net volume of the light-emitting area. This effect is less pronounced in InGaN QWs where carriers are effectively

localized at certain potential minima caused by In composition fluctuation in the QWs to form quantized excitons before being trapped in nonradiative pathways at TDs,[4–8] resulting in a markedly slow decay time (1–40 ns). The depth of these localized energy states with a small In composition fluctuation is enhanced by the large band-gap bowing of InGaN.[19] Assuming that the lateral spacing of the effective band-gap (potential) minimum determines the carrier diffusion length in InGaN, the carrier diffusion length was estimated to be less than 60 nm.[8] The absence of change in the Stokes-like shift due to the reduction of TD density revealed that the effective band-gap fluctuation in InGaN QWs is not due to a phase separation initiated by TDs.[20,21]

The localized states of an InGaN layer play a key role in the high efficiency only for LEDs. For LDs, InGaN has also been used as the active layer because laser oscillation using a GaN or an AlGaN active layer under current injection has not yet been achieved. Thus, for LDs, InGaN seems to play an important role in forming the localized states that lead to emission. However, the operating current density of the LD is one order higher than that of the LED. Therefore, in the InGaN active layer of LDs, some of the injected carriers easily overflow from the localized states formed by the In composition fluctuation, and they recombine nonradiatively at the nonradiative recombination centers formed by a large number of TDs. Furthermore, the localized excitons are easily screened by a large number of injected carriers. Considering these results, there is a possibility that a small amount of In mixed with GaN dramatically reduces the number of nonradiative recombination centers formed by point or nanopipe defects[22,23] and also forms the localized energy states due to In composition fluctuation.

Here, the present progress of InGaN-based LEDs is described, considering the role of the InGaN layer and referring to the previous works mentioned above.

2. InGaN-based UV/Blue/Green/Amber/Red LEDs

The reason why InGaN-based LEDs are so efficient despite having a large number of TDs has not yet been clarified.[15] However, there is a clue as to the reason. The high-efficiency LEDs can be obtained only by using an InGaN active layer for the LED and LDs. When the active layer of the LEDs is GaN or AlGaN, the efficiency of LEDs is considerably low.[11,12] The PL intensity of band-to-band emission of the GaN layer[24] is much weaker than that of the InGaN layer[25] when they are grown by MOCVD. Thus, the InGaN active layer is considered to be related to the high efficiency of the LEDs and LDs despite having a large number of TDs.

III-V nitride films were grown using the two-flow MOCVD method, the details of which have been described elsewhere.[26,27] The growth was conducted at atmospheric pressure. Sapphire with a (0001) orientation (C-face) and a two inch diameter was used as the substrate. The green LED device structures consisted of a 300 Å GaN buffer layer grown at a low temperature (550°C), a 5-μm-thick layer of n-type GaN:Si, a 30-Å-thick active layer of undoped $In_{0.45}Ga_{0.55}N$, a 600-Å-thick layer of p-type $Al_{0.2}Ga_{0.8}N$:Mg, and a 0.15-μm-thick layer of p-type GaN:Mg. The active region was a SQW structure consisting of a 30 Å $In_{0.45}Ga_{0.55}N$ well layer sandwiched by 5 μm n-type GaN and 600 Å p-type $Al_{0.2}Ga_{0.8}N$ barrier layers. The In composition of the InGaN well layer was nearly zero for UV LEDs[11,12] and 0.2 for blue LEDs.[10] Here, the In composition was determined assuming that the bowing parameter of InGaN was 1 eV.[28] However, recent studies revealed that the bowing parameter of InGaN is much higher than 1 eV.[19,29] In such a case, the In content in the InGaN layer should be much lower than the above values. For UV LEDs, the thickness of the undoped InGaN well layer was changed to 55 Å and an $Al_{0.2}Ga_{0.8}N$ barrier layer was used for both n- and p-type barrier layers. The fabrication of LED chips has been described in other papers.[26]

Figure 1 shows the emission spectra of various UV LEDs with different In compositions.[11,12] The intensity of the spectra of the UV LEDs containing a small amount of In in the active layer, with the emission wavelength of 383 nm was about 25-fold higher than that devoid of In with the emission wavelength of 368 nm. With decreasing In composition in the active layer, which means that the emission peak wavelength becomes shorter, the intensity of the spectra decreases dramatically. Thus, high-power UV LEDs can be obtained only when using an InGaN active layer with a relatively high In composition. This is related to the large localized energy states caused by In composition fluctuation in the InGaN well layer.[4–8] When electrons and holes are injected into the InGaN active layer of the LEDs, these carriers are captured by the localized energy states before they are captured by the nonradiative recombination centers which are caused by the large number of TDs. At these large localized energy states, localized excitons with a relatively high binding energy due to a quantum-well structure are formed and recombine radiatively. Without In in the active layer, there are no In composition fluctuations that generate the large localized energy state in the InGaN active layer. Thus, the quantum-confined Stark effect (QCSE) resulting from the piezoelectric field due to the strain becomes dominant.[30–33] This field, if strong enough, will induce a spatial separation of the electron and hole wave functions in the well. Then, the wave function overlap decreases and the in-

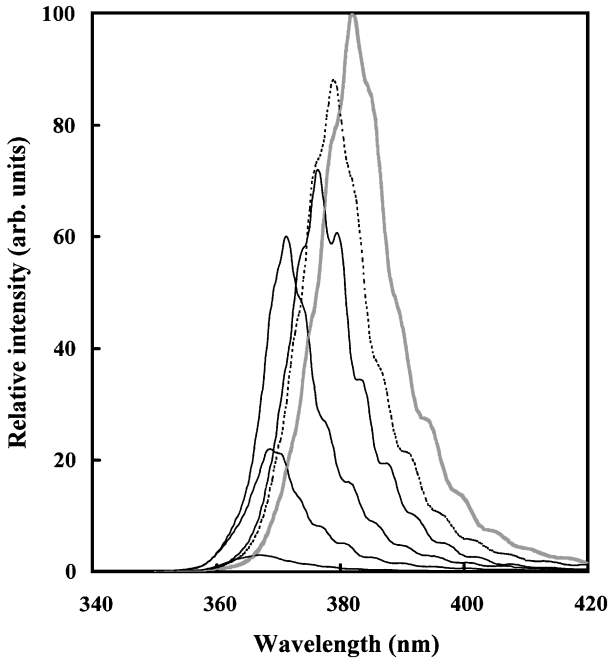

Fig. 1. Emission spectra of UV InGaN SQW LEDs with different In mole fractions in the active layer.

terband recombination rate is reduced. Also, there is no In composition fluctuation when carriers are captured by the localized energy states before they are captured by the nonradiative recombination centers. Thus, the efficiency of the UV LEDs becomes extremely low when the active layer is GaN or InGaN with a small amount of In, as shown in Fig. 1. When the emission peak wavelength becomes shorter than 371 nm, the output power decreases dramatically, probably due to the additional reason of a self-absorption of the light by n- and p-type GaN contact layers. Mayer *et al.*[34] previously reported the GaN-based UV LEDs had a large self-absorption of the emission light due to the GaN layer at wavelengths shorter than 370 nm. Figure 2 shows the relative output power of UV InGaN SQW LEDs as a function of emission peak wavelength with different In mole fractions in the active layer.

Next, amber LEDs were fabricated by increasing the In composition of the InGaN well layer. Figure 3 shows the emission spectrum of amber InGaN LEDs at a forward current of 20 mA at RT. For comparison, the spectra of commercially available amber and red AlInGaP LEDs fabricated on transparent substrates of GaP made by Hewlett-Packard[35] are also shown. The peak wavelength and the full-width at half maximum (FWHM) of the emission spectrum of the amber InGaN LEDs were 594 nm and 50 nm, respectively, and those of amber AlInGaP LEDs were 591 nm and 16 nm, respectively. The peak wavelength and the FWHM of the emission spectrum of red AlInGaP LEDs were 624 nm and 18 nm, respectively. The spectral width of the InGaN LEDs is relatively broad due to the QCSE and In composition fluctuation in the InGaN well layer. In view of the spectral width, the AlInGaP LEDs seem to have superior color purity. In regard to the practical application of LEDs, however, in the color range from red to yellow, it is difficult for the human eye to detect the difference in color caused by a spectral-width difference of 16 nm to 50 nm. The output power of amber InGaN and AlInGaP LEDs were 1.4 mW and 1.4 mW, respectively, at a current of 20 mA.

Figure 4 shows the output power of blue/green/amber InGaN and amber/red AlInGaP LEDs as a function of the ambient temperature from −30°C to +80°C. The output powers of blue/green/amber InGaN and amber/red AlInGaP LEDs at 25°C and a current of 20 mA were 7 mW, 5 mW, 1.4 mW, 1.4 mW and 3.2 mW, respectively. The output powers of blue/green InGaN LEDs were much higher that those of other LEDs. The output power of each LED was normalized to 1.0 at 25°C. When the ambient temperature was increased from RT to 80°C, the output power of amber AlInGaP LEDs decreased dramatically to half that at RT due to carrier over-

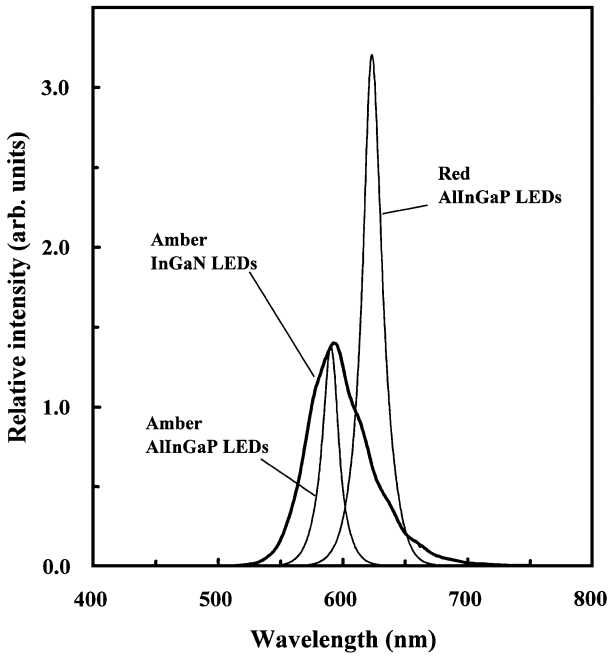

Fig. 3. Emission spectra of amber InGaN, amber AlInGaP and red AlInGaP LEDs at a forward current of 20 mA.

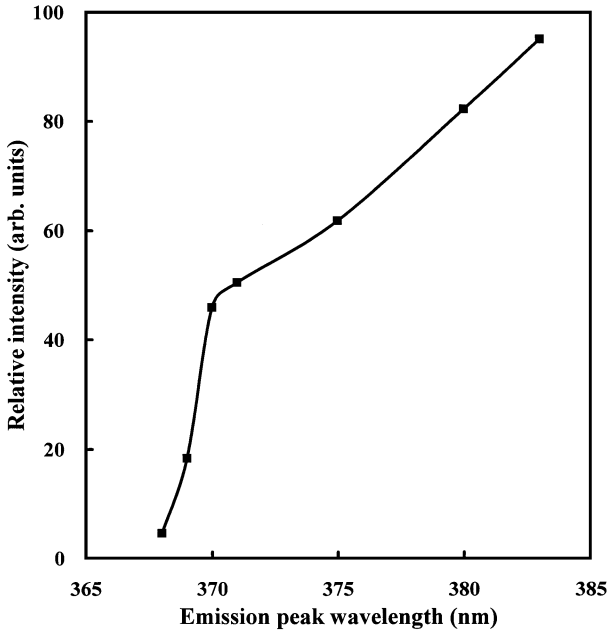

Fig. 2. Relative output power of UV InGaN SQW LEDs as a function of emission peak wavelength with different In mole fractions in the active layer.

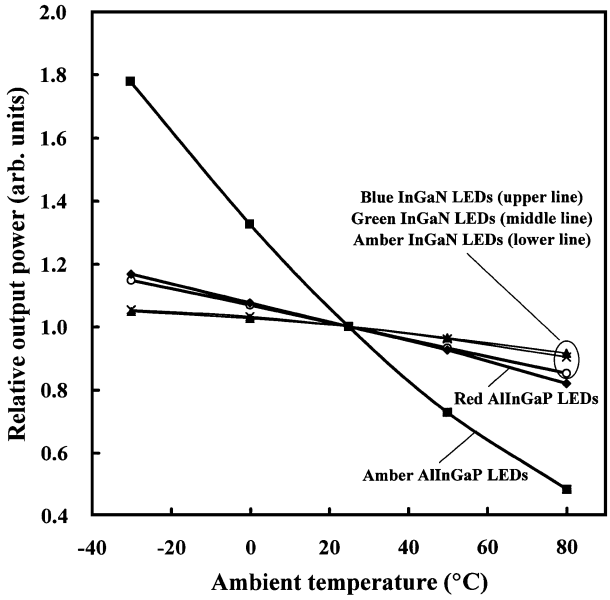

Fig. 4. Output power of blue/green/amber InGaN and amber/red AlInGaP LEDs as a function of the ambient temperature from −30°C to +80°C. The output power of each LED was normalized to 1.0 at 25°C.

flow caused by a small band offset between the active layer and cladding layers.[35] In the AlInGaP system, the band offset becomes much smaller with an increase of the band-gap energy of the active layer to the amber emission energy under a lattice-matched condition of the AlInGaP epilayer and GaAs substrate.[35] On the other hand, the temperature dependence of InGaN-based LEDs is relatively weak. When the ambient temperature is increased from RT to 80°C, the output power of amber InGaN LEDs only decreases to 90% of that at RT, probably due to a small carrier overflow caused by a large band offset between the active layer and cladding layers. The temperature dependence of blue/green InGaN-based LEDs and red AlInGaP LEDs is also shown. In the figure, InGaN-based LEDs show a smaller temperature dependence of the output power than that of conventional AlInGaP LEDs. In case of InGaN-based LEDs, the blue LEDs have the smallest temperature dependence among blue, green and amber LEDs. From the viewpoint of the band offset, however, the amber LEDs should have the smallest temperature dependence. Thus, other carrier transport mechanisms need to be considered to explain these temperature dependences of InGaN-based LEDs other than the band offset.

Red InGaN SQW LEDs were also fabricated by further increasing the In composition and thickness of InGaN well layers in the above LED structure. The In composition and thickness of the InGaN well layer were changed to approximately 50% and 60 Å, respectively. Here, the In composition was determined assuming that the bowing parameter of InGaN was 1 eV.[28] Figure 5 shows the emission spectrum of the red InGaN SQW LED at forward currents of 1 mA, 10 mA, 20 mA and 100 mA. At a current of 20 mA, the peak wavelength is 675 nm (1.84 eV), the peak emission energy of which is almost equal to the band-gap energy of InN (1.89 eV).[36] When the current was changed from 20 mA to 100 mA, a large blue shift of the peak wavelength was observed from 675 nm to 580 nm. At a current of 1 mA, the red emission suddenly disappeared. The reason why the intensity of the red emission decreased dramatically at a low current of 1 mA remains unknown. The output power of the red LED was as low as 0.3 mW at a current of 20 mA. There is a possibility that this red emission originates from the carrier recombinations at the deep energy levels of InGaN. Figure 6 shows the emission spectra of various InGaN LEDs with different In compositions. When the In composition was varied, the peak wavelength of the emission spectra of the LEDs changed continuously from the blue to red color region without any additional deep level emission. Thus, the red emission originates from the carrier recombination of band-to-band transition. There is an additional emission peak at a wavelength of around 470 nm, which probably originates from a low-In-composition InGaN formed via the phase separation of the InGaN well layer due to a high In composition of the well layer.[37] This additional emission peak of 470 nm also reflects the phase separation of the InGaN layer,[37] i.e., In composition fluctuation in the well layer. Considering these results, the dependence of the emission wavelength of the red LED on the current (blue shift) is dominated by both the band-filling effect of the localized energy states and the screening effect of the QCSE. The red emission originates from carrier recombinations at localized states caused by a high-In-composition InGaN formed via the phase separation of the InGaN well layer. The long wavelength emission of 675 nm can be explained by both effects of the localized states formed by InGaN phase separation and the QCSE. The blue shift of the electroluminescence (EL) of the red InGaN SQW LEDs with increasing operating current maybe explained only by the carrier screening of the QCSE resulting from piezoelectric fields[30–33] when the In composition and thickness of the InGaN well layer are large. However, a higher efficiency of the LEDs with increasing strain in the SQW upon increasing the In content in the InGaN well layers, was observed from UV to green LEDs, as shown in Figs. 1 and 7.[10–13,26] These results cannot be explained only by the carrier screening of the QCSE.

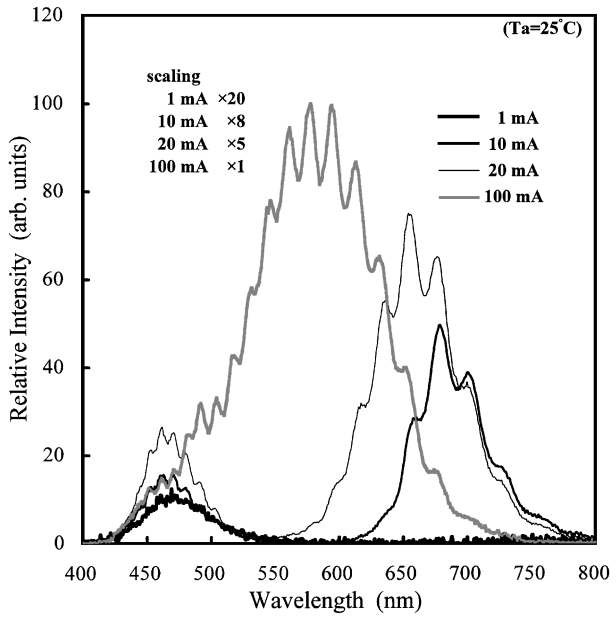

Fig. 5. Emission spectra of red InGaN SQW LEDs at different operating currents.

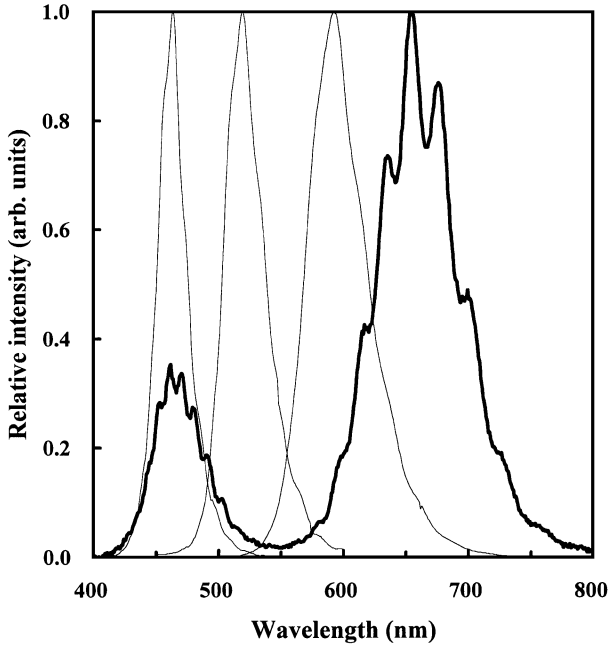

Fig. 6. Emission spectra of blue, green, amber and red InGaN LEDs.

Figure 7 shows the external quantum efficiency as a function of the emission wavelength of InGaN-based UV, blue, green, amber and red LEDs at forward currents of 1 and 20 mA. The blue and green LEDs have the highest efficiency of 14% and 11%, respectively, in spite of a large QCSE with a relatively strong stress due to a large lattice mismatch between the InGaN well layer and GaN barrier layers at 20 mA. At a low current of 1 mA, the green LEDs showed the highest external quantum efficiency of 18%. These phenomena cannot be explained by only the QCSE. It may be that the localization effects induced by In composition fluctuations must overcome these intrinsic limitations due to the piezoelectric field. The external quantum efficiency at 1 mA is much higher than that at 20 mA, which is probably related to the localized energy states. At a low current of 1 mA, the carrier overflow from the localized energy states where the carriers recombine radiatively is small. Thus, the efficiency of the LEDs is high at a low current. At a high current of 20 mA, some carriers overflow from the localized energy states and reach the nonradiative recombination centers formed by a large number of dislocations. Then the efficiency of the LEDs drops. In the longer wavelength region of amber and red colors, the efficiency becomes low mainly due to the QCSE which overcomes the effects of the localized energy states due to the large strain effects. At the shorter UV wavelength region, the efficiency also becomes low mainly due to the lack of localized energy states caused by In composition fluctuation. In Fig. 5, there is an additional emission peak at a wavelength of around 470 nm, which probably originates from a low-In-composition InGaN formed via the phase separation of the InGaN well layer due to a high In composition of the well layer.[37] This additional emission peak of 470 nm also reflects the phase separation of the InGaN layer,[37] i.e., In composition fluctuation in the well layer. Considering these results, the dependence of the emission wavelength of the red LED on the current (blue shift) is dominated by both the band-filling effect of the localized energy states and the screening effect of the QCSE.

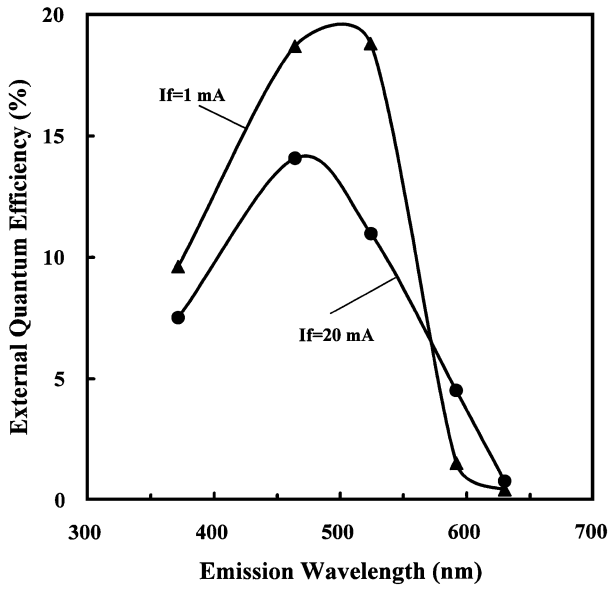

Fig. 7. External quantum efficiency as a function of the emission wavelength of InGaN-based UV, blue, green, amber and red LEDs.

Figure 8 shows the output power and external quantum efficiency of (a) blue and (b) green InGaN quantum-well-structure LEDs as a function of the forward current. The blue LED had the highest external quantum efficiency of 18% at a low current of 0.6 mA. The green LED had the highest efficiency of 20% at a low current of 0.1 mA. This dependence of the external quantum efficiency of blue and green LEDs on the current is probably related to the localized energy states. At a low current of around 0.1 mA, carrier overflow from the localized energy states where the carriers recombine radiatively is small. Thus, the efficiency of the LEDs is high at a low current. At a high current of 20 mA, some carriers can easily overflow from the localized energy states and reach the nonradiative recombination centers which are formed by a large number of dislocations. Then the efficiency of the LEDs

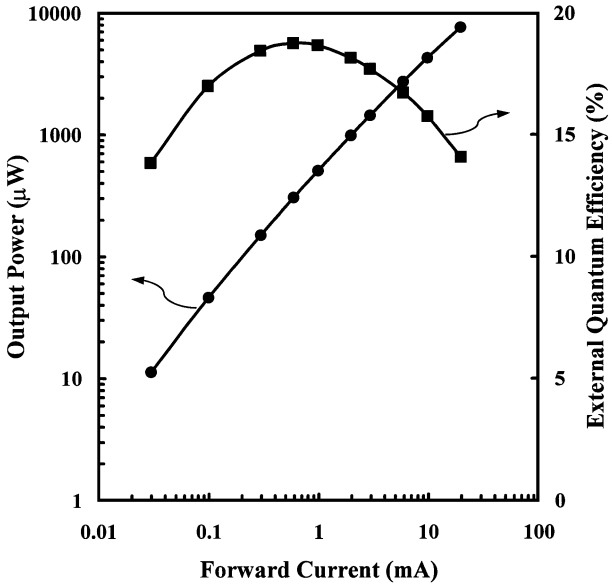

(a)

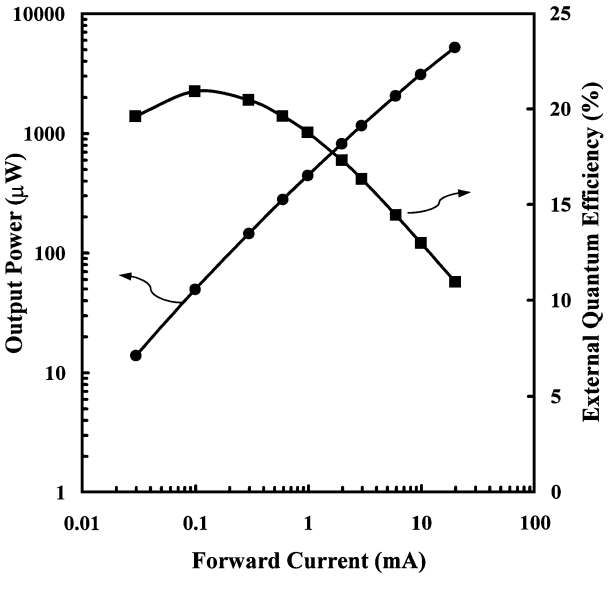

(b)

Fig. 8. The output power and the external quantum efficiency of (a) blue and (b) green InGaN quantum-well-structure LEDs as a function of the forward current.

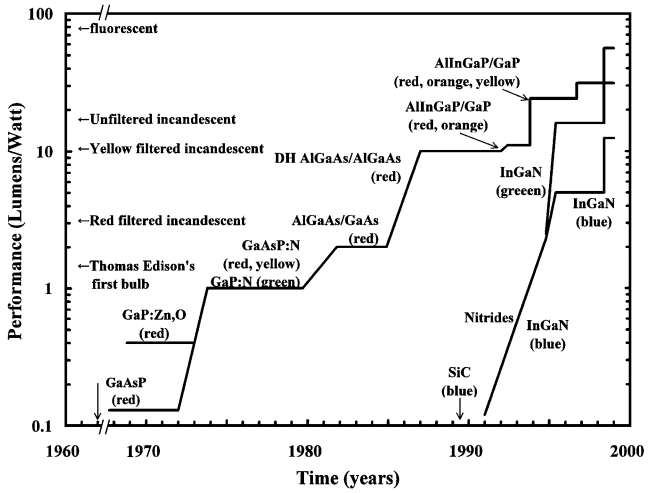

Fig. 9. The luminous efficiency of visible LEDs as a function of years of development.

drops.

Figure 9 shows the luminous efficiency of visible LEDs as a function of years of development,[38] where we have included the latest results of InGaN-based blue and green LEDs. Based on the figure, it is clearly seen that the speed of the progress of InGaN-based blue/green LEDs is exceptionally fast. Currently, the luminous efficiencies of green and blue InGaN-based LEDs are 60 and 13 lm/W, respectively, at low currents of 0.1 mA and 0.6 mA. That for red AlInGaP-based is 30 lm/W. These values of the luminous efficiency of the LEDs are much higher than that of the conventional incandescent bulbs. In order to save energy and natural resources, we must replace conventional incandescent bulbs with these LEDs. The luminous efficiency (60 lm/W) of green LEDs is close to that of a fluorescent light (80 lm/W), as shown in Fig. 9. Thus, there is the possibility of replacing conventional incandescent bulbs and fluorescent lights with LED all-solid-state light sources in the near future.

3. Conclusion

UV/blue/green/amber/red InGaN-based LEDs were obtained using an InGaN active layer instead of a GaN active layer. Red LEDs with an emission wavelength of 675 nm, the emission energy of which is almost equal to the band-gap energy of InN, were fabricated. The dependence of the emission wavelength of the red LED on the current (blue shift) is dominated by both the band-filling effect of the localized energy states and the screening effect of the piezoelectric field. In the red LEDs, a phase separation of the InGaN layer was clearly observed in the emission spectra, where blue and red emission peaks appeared. In terms of the output power and the temperature dependence of the LEDs, InGaN-based LEDs are superior to the conventional amber AlInGaP-based LEDs due to a large band offset between the active and cladding layers. The localized energy states caused by In composition fluctuation in the InGaN active layer contribute to the high efficiency of the InGaN-based LEDs despite the large number of dislocations and the large QCSE. Considering the previous results, the carrier diffusion length, determined by the potential fluctuation due to InGaN phase separation, must be less than the dislocation spacing in the InGaN layer in order to obtain high-efficiency InGaN-based LEDs.

1) S. Nakamura and T. Mukai: Jpn. J. Appl. Phys. **31** (1992) L1457.
2) S. Nakamura, M. Senoh and T. Mukai: Jpn. J. Appl. Phys. **32** (1993) L8.
3) S. Nakamura, T. Mukai, M. Senoh, S. Nagahama and N. Iwasa: J. Appl. Phys. **74** (1993) 3911.
4) S. Chichibu, T. Azuhata, T. Sota and S. Nakamura: Appl. Phys. Lett. **69** (1996) 4188.
5) S. Chichibu, T. Azuhata, T. Sota and S. Nakamura: Appl. Phys. Lett. **70** (1997) 2822.
6) Y. Narukawa, Y. Kawakami, Sz. Fujita, Sg. Fujita and S. Nakamura: Phys. Rev. B **55** (1997) 1938R.
7) Y. Narukawa, Y. Kawakami, M. Funato, Sz. Fujita, Sg. Fujita and S. Nakamura: Appl. Phys. Lett. **70** (1997) 981.
8) S. Chichibu, K. Wada and S. Nakamura: Appl. Phys. Lett. **71** (1997) 2346.
9) S. Nakamura, T. Mukai and M. Senoh: Appl. Phys. Lett. **64** (1994) 1687.
10) S. Nakamura, M. Senoh, N. Iwasa, S. Nagahama, T. Yamada and T. Mukai: Jpn. J. Appl. Phys. **34** (1995) L1332.
11) T. Mukai, D. Morita and S. Nakamura: J. Cryst. Growth **189/190** (1998) 778.
12) T. Mukai, M. Yamada and S. Nakamura: Jpn. J. Appl. Phys. **37** (1998) L1358.
13) T. Mukai, H. Narimatsu and S. Nakamura: Jpn. J. Appl. Phys. **37** (1998) L479.
14) S. Nakamura, M. Senoh, S. Nagahama, N. Iwasa, T. Yamada, T. Matsushita, H. Kiyoku and Y. Sugimoto: Jpn. J. Appl. Phys. **35** (1996) L74.
15) S. D. Lester, F. A. Ponce, M. G. Crawford and D. A. Steigerwald: Appl. Phys. Lett. **66** (1995) 1249.
16) D. Kapolnek, X. H. Wu, B. Heying, S. Keller, B. Keller, U. K. Mishra, S. P. Denbaars and J. S. Speck: Appl. Phys. Lett. **67** (1995) 1541.
17) X. H. Wu, P. Fini, S. Keller, E. J. Tarsa, B. Heying, U. K. Mishra, S. P. DenBaars and J. S. Speck: Jpn. J. Appl. Phys. **35** (1996) L1648.
18) S. Chichibu, H. Marchand, M. S. Minsky, S. Keller, P. T. Fini, J. P. Ibbetson, S. B. Fleischer, J. S. Speck, J. E. Bowers, E. Hu, U. K. Mishra, S. P. Denbaars, T. Deguchi, T. Sota and S. Nakamura: Appl. Phys. Lett. **74** (1999) 1460.
19) M. D. McCluskey, C. G. Van de Walle, C. P. Master, L. T. Romano and N. M. Johnson: Appl. Phys. Lett. **72** (1998) 2725.
20) H. Sato, T. Sugahara, Y. Naoi and S. Sakai: Jpn. J. Appl. Phys. **37** (1998) 2013.
21) S. Keller, U. K. Mishra, S. P. Denbaars and W. Seifert: Jpn. J. Appl. Phys. **37** (1998) L431.
22) E. J. Tarsa, B. Heying, X. H. Wu, P. Fini, S. P. Denbaars and J. S. Speck: J. Appl. Phys. **82** (1997) 5472.
23) F. A. Ponce, D. P. Bour, W. Gotz and P. J. Wright: Appl. Phys. Lett. **68** (1996) 57.
24) S. Nakamura, T. Mukai and M. Senoh: Jpn. J. Appl. Phys. **31** (1992) 2883.
25) S. Nakamura, T. Mukai and M. Senoh: Jpn. J. Appl. Phys. **32** (1993) L16.
26) S. Nakamura and G. Fasol: *The Blue Laser Diode* (Springer-Verlag, Heidelberg, 1997) 1st ed.
27) S. Nakamura: Jpn. J. Appl. Phys. **30** (1991) L1705.
28) S. Nakamura: Microelectron. J. **25** (1994) 651.
29) T. Takeuchi, H. Takeuchi, S. Sota, H. Sakai, H. Amano and I. Akasaki: Jpn. J. Appl. Phys. **36** (1997) L177.
30) T. Takeuchi, S. Sota, M. Katsuragawa, M. Komori, H. Takeuchi, H. Amano and I. Akasaki: Jpn. J. Appl. Phys. **36** (1997) L382.
31) D. L. Smith and C. Mailhiot: Phys. Rev. Lett. **58** (1987) 1264.
32) M. B. Nardelli, K. Rapcewicz and J. Bernholc: Appl. Phys. Lett. **71** (1997) 3135.
33) J. S. Im, H. Kollmer, J. Off, A. Sohmer, F. Scholz and A. Hangleiter: Phys. Rev. B **57** (1998) R9435.
34) M. Mayer, A. Pelzmann, C. Kirchner, M. Schauler, F. Eberhard, M. Kamp, P. Unger and K. J. Ebeling: J. Cryst. Growth **189/190** (1998) 782.
35) F. A. Kish and R. M. Fletcher: *AlInGaP Light-Emitting Diodes*, eds. G. B. Stringfellow and M. G. Crawford (Academic Press, San Diego, 1997) Semiconductors and Semimetals, Vol. 48, Chap. 5, p. 149.
36) S. Strite and H. Morkoc: J. Vac. Sci & Technol. B **10** (1992) 1237.
37) I. Ho and G. B. Stringfellow: Appl. Phys. Lett. **69** (1996) 2701.
38) F. A. Ponce and D. P. Bour: Nature **386** (1997) 351.